Australopithecus sediba: A New Species of *Homo*-Like Australopith from South Africa

Lee R. Berger,[1,2]* Darryl J. de Ruiter,[3,1] Steven E. Churchill,[4,1] Peter Schmid,[5,1] Kristian J. Carlson,[1,6] Paul H. G. M. Dirks,[2,7] Job M. Kibii[1]

Despite a rich African Plio-Pleistocene hominin fossil record, the ancestry of *Homo* and its relation to earlier australopithecines remain unresolved. Here we report on two partial skeletons with an age of 1.95 to 1.78 million years. The fossils were encased in cave deposits at the Malapa site in South Africa. The skeletons were found close together and are directly associated with craniodental remains. Together they represent a new species of *Australopithecus* that is probably descended from *Australopithecus africanus*. Combined craniodental and postcranial evidence demonstrates that this new species shares more derived features with early *Homo* than any other australopith species and thus might help reveal the ancestor of that genus.

The origin of the genus *Homo* is widely debated, with several candidate ancestors being proposed in the genus *Australopithecus* (*1*–*3*) or perhaps *Kenyanthropus* (*4*). The earliest occurrence of fossils attributed to *Homo* (*H.* aff. *H. habilis*) at 2.33 million years ago (Ma) in Ethiopia (*5*) makes it temporally antecedent to all other known species of the genus *Homo*. Within early *Homo*, the hypodigms and phylogenetic relationships between *H. habilis* and another early species, *H. rudolfensis*, remain unresolved (*6*–*8*), and the placement of these species within *Homo* has been challenged (*9*). *H. habilis* is generally thought to be the ancestor of *H. erectus* (*10*–*13*), although this might be questioned on the basis of the considerable temporal overlap that existed between them (*14*). The identity of the direct ancestor of the genus *Homo*, and thus its link to earlier *Australopithecus*, remains controversial. Here we describe two recently discovered, directly associated, partially articulated *Australopithecus* skeletons from the Malapa site in South Africa, which allow us to investigate several competing hypotheses regarding the ancestry of *Homo*. These skeletons cannot be accommodated within any existing fossil taxon; thus, we establish a new species, *Australopithecus sediba*, on the basis of a combination of primitive and derived characters of the cranium and postcranium.

The following is a description of *Au. sediba*: Order Primates Linnaeus 1758; suborder Anthropoidea Mivart 1864; superfamily Hominoidea Gray 1825; family Hominidae Gray 1825; genus *Australopithecus* DART 1925; species *Australopithecus sediba* sp. nov.

Etymology. The word *sediba* means "fountain" or "wellspring" in the seSotho language.

Holotype and paratype. Malapa Hominin 1 (MH1) is a juvenile individual represented by a partial cranium, fragmented mandible, and partial postcranial skeleton that we designate as the species holotype [Figs. 1 and 2, supporting online material (SOM) text S1, figs. S1 and S2, and table S1]. The first hominin specimen recovered from Malapa was the right clavicle of MH1 (UW88-1), discovered by Matthew Berger on 15 August 2008. MH2 is an adult individual represented by isolated maxillary teeth, a partial mandible, and partial postcranial skeleton that we designate as the species paratype. Although MH1 is a juvenile, the second molars are already erupted and in occlusion. Using either a human or an ape model, this indicates that MH1 had probably attained at least 95% of adult brain size (*15*). Although additional growth would have occurred in the skull and skeleton of this individual, we judge that it would not have appreciably altered the morphology on which this diagnosis is based.

Locality. The two *Au. sediba* type skeletons were recovered from the Malapa site (meaning "homestead" in seSotho), situated roughly 15 km NNE of the well-known sites of Sterkfontein, Swartkrans, and Kromdraai in Gauteng Province, South Africa. Detailed information regarding geology and dating of the site is in (*16*).

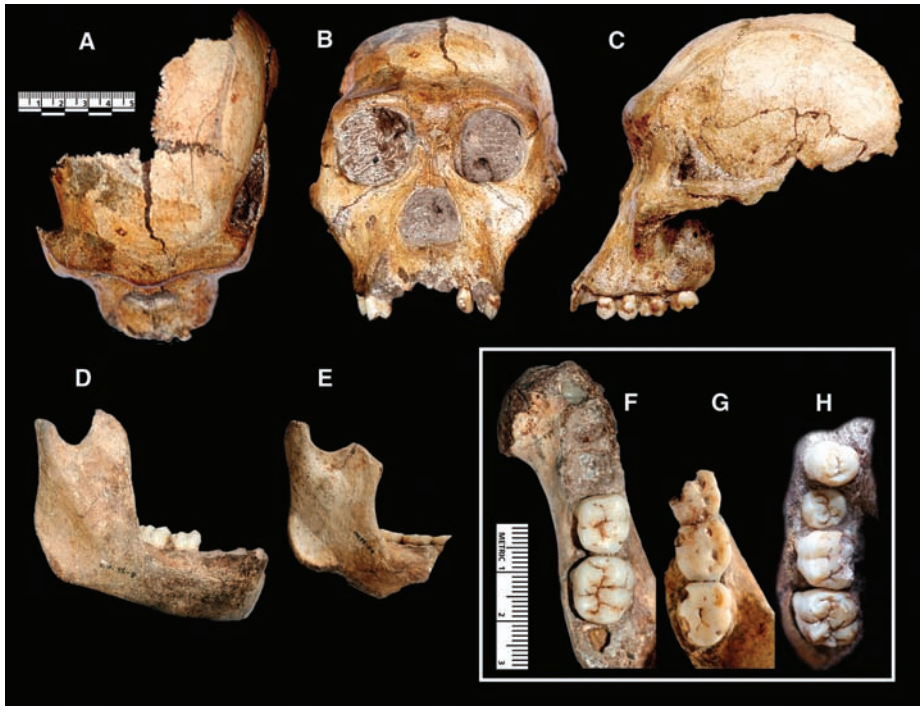

Fig. 1. Craniodental elements of *Au. sediba.* UW88-50 (MH1) juvenile cranium in (**A**) superior, (**B**) frontal, and (**C**) left lateral views. (**D**) UW88-8 (MH1) juvenile mandible in right lateral view, (**E**) UW88-54 (MH2) adult mandible in right lateral view, (**F**) UW88-8 mandible in occlusal view, (**G**) UW 88-54 mandible in occlusal view, and (**H**) UW 88-50 right maxilla in occlusal view (scale bars are in centimeters).

[1]Institute for Human Evolution, University of the Witwatersrand, Private Bag 3, Wits 2050, South Africa. [2]School of Geosciences, University of the Witwatersrand, Private Bag 3, Wits 2050, South Africa. [3]Department of Anthropology, Texas A&M University, College Station, TX 77843, USA. [4]Department of Evolutionary Anthropology, Box 90383, Duke University, Durham, NC 27708, USA. [5]Anthropological Institute and Museum, University of Zürich, Winterthurerstrasse 190, CH-8057 Zürich, Switzerland. [6]Department of Anthropology, Indiana University, Bloomington, IN 47405, USA. [7]School of Earth and Environmental Sciences, James Cook University, Townsville, Queensland 4811, Australia.

*To whom correspondence should be addressed. E-mail: profleeberger@yahoo.com

Diagnosis. *Au. sediba* can be distinguished from other species of *Australopithecus* by a combination of characters presented in Table 1; comparative cranial measures are presented in Table 2. A number of derived characters separate *Au. sediba* from the older chronospecies *Au. anamensis* and *Au. afarensis*. *Au. sediba* exhibits neither the extreme megadontia, extensive cranial cresting, nor facial prognathism of *Au. garhi*. The suite of derived features characterizing *Au. aethiopicus*, *Au. boisei*, and *Au. robustus*, in particular the pronounced cranial muscle markings, derived facial morphology, mandibular corpus robusticity, and postcanine megadontia, are absent in *Au. sediba*. The closest morphological comparison for *Au. sediba* is *Au. africanus*, as these taxa share numerous similarities in the cranial vault, facial skeleton, mandible, and teeth (Table 1). Nevertheless, *Au. sediba* can be readily differentiated from *Au. africanus* on both craniodental and postcranial evidence. Among the more notable differences, we observe that although the cranium is small, the vault is relatively transversely expanded with vertically oriented parietal walls and widely spaced temporal lines; the face lacks the pronounced, flaring zygomatics of *Au. africanus*; the arrangement of the supraorbital torus, nasoalveolar region, infraorbital region, and zygomatics result in a derived facial mask; the mandibular symphysis is vertically oriented with a slight bony chin and a weak post-incisive planum; and the teeth are differentiated by the weakly defined buccal grooves of the maxillary premolars, the weakly developed median lingual ridge of the mandibular canine, and the small absolute size of the postcanine dentition. These exact differences also align *Au. sediba* with the genus *Homo* (see SOM text S2 for hypodigms used in this study). However, we consider *Au. sediba* to be more appropriately positioned within *Australopithecus*, based on the following craniodental features: small cranial capacity, pronounced glabelar region, patent premaxillary suture, moderate canine jugum with canine fossa, small anterior nasal spine, steeply inclined zygomaticoalveolar crest, high masseter origin, moderate development of the mesial marginal ridge of the maxillary central incisor, and relatively closely spaced premolar and molar cusps.

Postcranially, *Au. sediba* is similar to other australopiths in its small body size, its relatively long upper limbs with large joint surfaces, and the retention of apparently primitive characteristics in the upper and lower limbs (table S2). *Au. sediba* differs from other australopiths, but shares with *Homo* a number of derived features of the os coxa, including increased buttressing of the ilium and expansion of its posterior portion, relative reduction in the distance between the sacroiliac and hip joints, and reduction of distance from the acetabulum to the ischial tuberosity. These synapomorphies with *Homo* anticipate the reorganization of the pelvis and lower limb in *H. erectus* and possibly the emergence of more energetically efficient walking and running in that taxon (*17*). As with the associated cranial remains, the postcranium of *Au. sediba* is defined not by the presence of autapomorphic features but by a unique combination of primitive and derived traits.

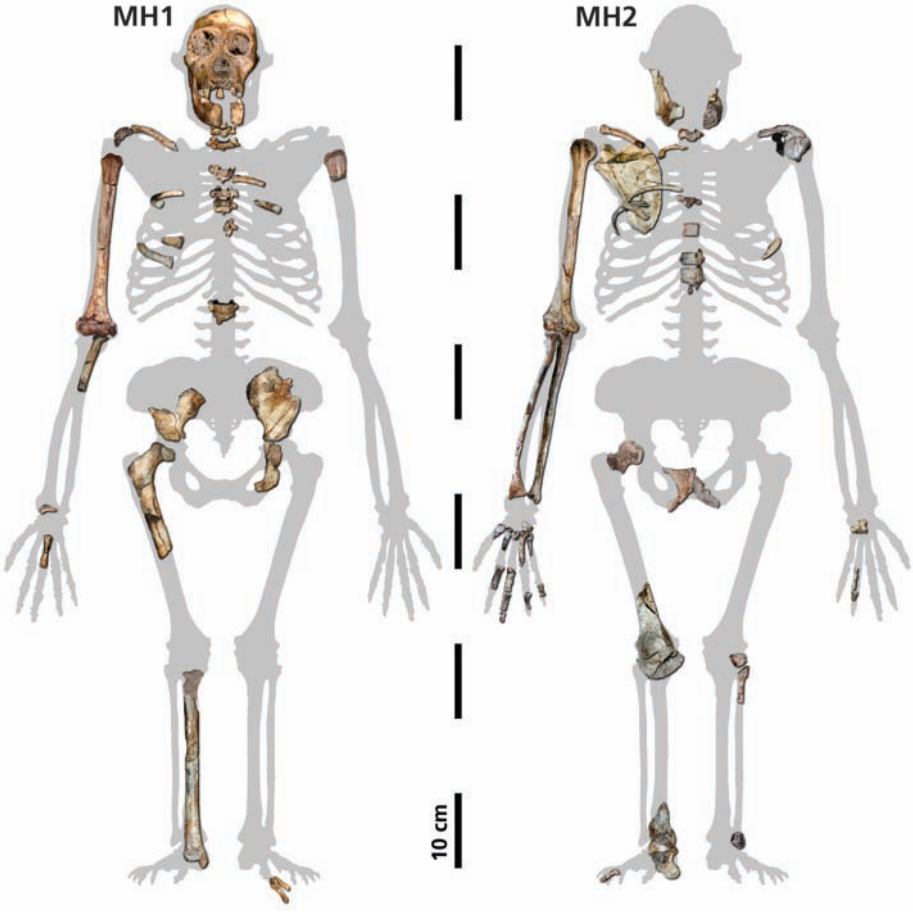

Fig. 2. Associated skeletal elements of MH1 (**left**) and MH2 (**right**), in approximate anatomical position, superimposed over an illustration of an idealized *Au. africanus* skeleton (with some adjustment for differences in body proportions). The proximal right tibia of MH1 has been reconstructed from a natural cast of the proximal metaphysis.

Cranium. The cranium is fragmented and slightly distorted. The minimum cranial capacity of MH1 is estimated at 420 cm^3 (SOM text S4). The vault is ovoid, with transversely expanded, vertically oriented parietal walls. The widely spaced temporal lines do not approach the midline. Postorbital constriction is slight. The weakly arched supraorbital torus is moderately developed and laterally extended, with sharply angled lateral corners and a weakly defined supratoral sulcus. A robust glabelar region is evident, with only a faint depression of the supraorbital torus at the midline. The frontal process of the zygomatic faces primarily laterally and is expanded medially but not laterally. The zygomatic prominence does not show anterolateral expansion. The zygomatics are weakly flared laterally, resulting in an uninterrupted frontal profile of the facial mask that is squared superiorly and tapered inferiorly. The zygomaticoalveolar crests are long, straight, and steeply inclined, resulting in a high masseter origin. The root of the zygomatic begins at the anterior margin of M^1. The nasal bones are widened superiorly, become narrowest about one-third of the way down, and flare to their widest extent at their inferior margin. The nasal bones are elevated as a prominent ridge at the internasal suture, with an increasingly anterior projection inferiorly. The bone surface of the maxilla retreats gently away from the nasal aperture laterally, resulting in an everted margin of the superolateral portion of the aperture relative to the infraorbital region. The inferolateral portion of the nasal aperture becomes bluntly rounded. The infraorbital region is slightly convex (*18*) and is oriented at an approximately right angle to the alveolar plane. There is a trace of a premaxillary suture near the superolateral margin of the nasal aperture. Prominent canine juga delineate moderately developed canine fossae. Anterior pillars are absent. The inferior margin of the nasal aperture is marked by a stepped nasal sill and a small but distinct anterior nasal spine. The subnasal region is straight in the coronal plane and only weakly projecting relative

Table 1. List of characters used to diagnose *Au. sediba*. These characters are commonly used in hominin phylogenetic studies (*11, 38–40*) or have been recorded as diagnostic for various hominin taxa in the past (*3*, *10*, *36*). Recognizing the potential pitfalls of performing a cladistic analysis on possibly interdependent characters of uncertain valence, we produced a cladogram from the data in this table as a test of the phylogenetic position of *Au. sediba* (fig. S3). Our most parsimonious cladogram places *Au. sediba* at the stem of the *Homo* clade. Numbers in parentheses in the first column refer to measures presented in Table 2; descriptions of these character states are provided in SOM text S3. Abbreviations are as follows: A-M, anteromedial; costa supr., costa supraorbitalis; intermed., intermediate; lat., lateral; med., medial; mesognath., mesognathic; mod., moderately; MMR, mesial marginal ridge; orthogn., orthognathic; procumb., procumbent; proj., projecting; TMJ, temperomandibular joint.

Characters	*Au. afarensis*	*Au. garhi*	*Au. africanus*	*Au. sediba*	*H. habilis*	*H. rudolfensis*	*H. erectus*	*Au. aethiopicus*	*Au. boisei*	*Au. robustus*
Vault										
Cranial capacity (1)	Small	Small	Small	Small	Intermed.	Large	Large	Small	Small	Small
A-M incursion of temporal lines on frontal bone (9)	Strong	Moderate	Moderate	Weak	Weak	Weak	Weak	Strong	Strong	Strong
Position of temporal lines on parietal bones	Crest	Crest	Variable	Wide	Variable	Wide	Wide	Crest	Crest	Crest
Compound temporal nuchal crest (males)	Extensive	?	Absent	Absent	Variable	Absent	Absent	Extensive	Variable	Absent
Postorbital constriction (5)	Marked	Moderate	Moderate	Slight	Moderate	Moderate	Slight	Marked	Marked	Marked
Pneumatization of temporal squama	Extensive	?	Extensive	Reduced	Reduced	Reduced	Reduced	Extensive	Variable	Reduced
Facial hafting	Low	Low	Low	Low	Low	Low	Low	High	High	High
Frontal trigon	Present	Present	Absent	Absent	Absent	Absent	Absent	Present	Present	Present
Supraglenoid gutter width	Narrow	?	Narrow	Narrow	Narrow	Narrow	Narrow	Wide	Wide	Wide
Horizontal distance between TMJ and M2/M3 (6)	Long	?	Long	Short	Short	Long	Short	Long	Long	Long
Parietal transverse expansion/tuber	Absent	Absent	Absent	Present	Present	Present	Present	Absent	Absent	Absent
Facial skeleton										
Supraorbital expression	Costa supr.	Costa supr.	Intermed.	Torus	Torus	Intermed.	Torus	Costa supr.	Costa supr.	Costa supr.
Supraorbital contour	Less arched	Less arched	Variable	Arched	Arched	Arched	Arched	Less arched	Variable	Arched
Glabellar region forms as prominent block	No	No	Variable	Yes	No	Variable	No	No	Yes	Yes
Lat. half of infraorbital margin blunt and protruding	No	?	No	No	No	No	No	Yes	No	Yes
Zygomatic arch relative to inferior orbital margin	Above	?	Level	Level	Level	?	Level	Above	Above	Above
Convexity/concavity of infraorbital region	?	?	Convex	Convex	Concave	Concave	Convex	Concave	Concave	Concave
Nasal bone projection above frontomaxillary suture	Expanded	?	Variable	No	No	No	No	Tapered	Expanded	Expanded
Inferior width of projecting nasal bone (25)	Wide	?	Variable	Wide	Variable	Narrow	Wide	Not proj.	Not proj.	Not proj.
Infraorbital foramen height (32)	High	?	Variable	High	High	?	High	Low	Low	Low

continued on next page

Characters	*Au. afarensis*	*Au. garhi*	*Au. africanus*	*Au. sediba*	*H. habilis*	*H. rudolfensis*	*H. erectus*	*Au. aethiopicus*	*Au. boisei*	*Au. robustus*
Canine juga prominence/anterior pillars	Prominent	Prominent	Variable	Prominent	Variable	Weak	Weak	Weak	Weak	Pillars
Patency of premaxillary suture	Obliterated	?	Occasional	Trace	Obliterated	Obliterated	Obliterated	Obliterated	Obliterated	Occasional
Inferolateral nasal aperture margin	Sharp	Sharp	Variable	Blunt	Variable	Sharp	Blunt	Blunt	Variable	Blunt
Eversion of superior nasal aperture margin	?	?	None	Slight	Slight	Slight	Slight	Slight	Variable	None
Nasoalveolar triangular frame/gutter	Triangular	?	Triangular	Triangular	Triangular	Triangular	Triangular	Gutter	Gutter	Gutter
Nasal cavity entrance	Stepped	Stepped	Stepped	Stepped	Variable	Stepped	Stepped	Smooth	Smooth	Smooth
Nasoalveolar clivus contour in coronal plane	Convex	Convex	Straight	Straight	Straight	Straight	Straight	Concave	Concave	Concave
Subnasal projection (38)	Marked	Marked	Variable	Weak	Variable	Weak	Weak	Marked	Moderate	Moderate
Canine fossa	Present	Present	Present	Present	Present	Absent	Absent	Absent	Absent	Absent
Maxillary fossula	Absent	Absent	Absent	Absent	Absent	Absent	Absent	Absent	Absent	Present
Incisor procumbency	Procumb.	Procumb.	Variable	Vertical	Variable	Vertical	Vertical	Vertical	Vertical	Vertical
Anterior nasal spine rel. to nasal aperture	Absent	?	Anterior	Anterior	Anterior	?	Enlarged	Posterior	Posterior	Posterior
Expansion of frontal process of zygomatic bone	Med. and lat.	?	Med. and lat.	Medial	Medial	Medial	Medial	Med. and lat.	Med. and lat.	Med. and lat.
Angular indentation of lateral orbital margin	?	?	Indented	Curved	Curved	Curved	Curved	?	Curved	Curved
Zygomatic prominence development	Prominent	?	Prominent	Slight	Slight	?	Slight	Prominent	Prominent	Prominent
Lateral flaring of zygomatic arches	Marked	?	Marked	Slight	Slight	Slight	Slight	Marked	Marked	Marked
Outline of superior facial mask	Tapered	?	Tapered	Squared	Squared	Squared	Squared	Tapered	Tapered	Tapered
Zygomaticoalveolar crest/malar notch	Straight	?	Straight	Straight	Notch	Notch	Notch	Straight	Straight	Straight
Infraorbital plate angle relative to alveolar plane	Obtuse	?	Obtuse	Right	Right	Right	Right	Obtuse	Obtuse	Obtuse
Zygomaticomaxillary steps and fossae present	No	?	No	No	No	No	No	No	No	Yes
Height of masseter origin (35)	Low	Low	High	High	Low	Low	Low	High	High	High
Malar thickness (31)	Thin	?	Thin	Thin	Thin	?	Thin	Thick	Thick	Thick
Projection of zygomatics relative to nasal bones	Posterior	Posterior	Variable	Posterior	Posterior	Level	Posterior	Anterior	Anterior	Anterior
Facial prognathism (7) (sellion-prosthion angle)	Prognathic	Prognathic	Variable	Mesognath.	Mesognath.	Mesognath.	Orthogn.	Prognathic	Mesognath.	Mesognath.
Masseteric position relative to sellion	Anterior	?	Posterior	Posterior	Posterior	?	Posterior	Anterior	Anterior	Anterior
Lateral anterior facial contour	Bipartite	Bipartite	Variable	Straight	Variable	Straight	Straight	Straight	Straight	Straight

Characters	*Au. afarensis*	*Au. garhi*	*Au. africanus*	*Au. sediba*	*H. habilis*	*H. rudolfensis*	*H. erectus*	*Au. aethiopicus*	*Au. boisei*	*Au. robustus*
Palate										
Protrusion of incisors beyond bi-canine line	Yes	Yes	Yes	Yes	Yes	No	Yes	No	No	No
Anterior palatal depth	Shallow	Shallow	Deep	Deep	Variable	Deep	Variable	Shallow	Deep	Shallow
Dental arcade shape	Rectangle	Rectangle	Variable	Parabolic	Parabolic	Parabolic	Parabolic	Rectangle	Parabolic	Parabolic
Maxillary I2/C diastema	Present	Present	Absent	Absent	Variable	Absent	Absent	Absent	Absent	Absent
Mandible										
Orientation of mandibular symphysis	Receding	?	Receding	Vertical	Vertical	Vertical	Vertical	Vertical	Vertical	Vertical
Bony chin (*mentum osseum*)	Absent	?	Slight	Slight	Slight	Slight	Slight	Slight	Slight	Slight
Direction of mental foramen opening	Variable	?	Variable	Lateral	Lateral	Lateral	Lateral	Lateral	Lateral	Lateral
Post-incisive planum	Prominent	?	Prominent	Weak	Prominent	Weak	Weak	Prominent	Prominent	Prominent
Torus marginalis and marginal tubercles	Prominent	?	Moderate	Moderate	Moderate	Prominent	Prominent	?	Prominent	Prominent
Mandibular corpus cross-sectional area at M_1 (50)	Small	?	Small	Small	Small	Variable	Small	Large	Large	Large
Teeth										
Incisor-to-postcanine ratio (maxillary) (60)	Large	Moderate	Moderate	Moderate	Moderate	Moderate	Large	?	Small	Small
Canine-to-postcanine ratio (maxillary/mandibular) (61, 62)	Large	Large	Large	Large	Large	Large	Large	?	Small	Small
Postcanine crown area (maxillary/mandibular) (57, 59)	Moderate	Large	Large	Moderate	Moderate	Large	Small	Large	Large	Large
Maxillary I^1: MMR development, lingual face	Moderate	?	Moderate	Moderate	Weak	Weak	Weak	?	Moderate	Moderate
Maxillary C: development of lingual ridges	Marked	Marked	Marked	Weak	Weak	Marked	Marked	?	Marked	Weak
Maxillary premolar molarization	None	Minor	Minor	None	Minor	Minor	None	Marked	Marked	Marked
Maxillary premolars: buccal grooves	Marked	Marked	Marked	Weak	Weak	Marked	Weak	?	Weak	Weak
Median lingual ridge of mandibular canine	Prom.	?	Prom.	Weak	Weak	Weak	Weak	?	Weak	Weak
Mandibular P_3 root number	2	?	2	2	1	2	1	?	2	2
Protoconid/metaconid more mesial cusp (molars)	Equal	?	Equal	Protoconid	Protoconid	Protoconid	Protoconid	?	Equal	Equal
Peak of enamel forms between roots of molars	No	?	Yes	Yes	No	No	No	?	No	Yes
Relative enamel thickness	Thick	Thick	Thick	Thick	Thick	Thick	Thick	Hyper	Hyper	Hyper
Positions of apices of lingual (LC) and buccal (BC) cusps of premolars and molars relative to occlusal margin	LC at margin, BC slightly lingual	LC at margin, BC slightly lingual	LC slightly buccal, BC moderately lingual	LC slightly buccal, BC moderately lingual	LC at margin, BC slightly lingual	LC at margin, BC slightly lingual	LC at margin, BC slightly lingual	LC mod. buccal, BC strongly lingual	LC mod. buccal, BC strongly lingual	LC mod. buccal, BC strongly lingual

Table 2. Craniodental measurements for early hominins in Africa. *Au. sediba* is represented by MH1. Unless otherwise defined, measurements are based on (*6*). Some measures were unavailable for specimens of *Au. afarensis* and *Au. garhi*, in which case the character states in Table 1 were estimated. Several character states in Table 1 are recorded as variable, although only species average values are presented here. Measurements are in millimeters unless otherwise indicated. Descriptions of character states presented in Table 1 that are based on measurements from this table are provided in SOM text S3. Abbreviations are as follows: br, bregma; ek, ectoconchion; ekm, ectomolare; fmt, frontomolare temporale; ft, frontotemporale; g, glabella; mf, maxillofrontale; n, nasion; ns, nasospinale; or, orbitale; po, porion; pr, prosthion; rhi, rhinion; zm, zygomaxillare; zy, zygion; zyo, zygoorbitale.

Item	Measurement description in (*6*)	Measurement	*Au. afarensis*	*Au. africanus*	*Au. sediba*	*H. habilis*	*H. rudolfensis*	*H. erectus*	*Au. aethiopicus*	*Au. boisei*	*Au. robustus*
1		Cranial capacity (cm^3)	415	442	420	631	751	900	419	515	530
2	9	Maximum parietal breadth	90	99	100	103	114	126	94	99	100
3	11	Bi-porionic breadth (po-po)	126	99	104	104	127	121	125	116	—
4		Postorbital constriction (narrowest point behind the orbits)	77	69	73	76	85	89	65	64	73
5		Postorbital constriction index (4/14 × 100)	66	71	85	70	72	80	65	61	68
6		Horizontal distance between TMJ and M^2/M^3	83	61	45	51	58	57	94	82	81
7		Facial prognathism (sellion-prosthion angle)	63	61	65	65	68	72	41	66	69
8	75	Infratemporal fossa depth	–	31	21	27	–	37	51	50	36
9	8	Minimum frontal breadth (ft-ft)	40	54	70	66	72	76	33	36	35
10	17	Glabella to bregma (g-br)	101	80	75	83	86	103	–	87	–
11		Frontal chord (n-br)	–	84	74	80	93	99	–	84	–
12	62	Supraorbital torus vertical thickness	–	8	8	8	10	12	10	12	9
13	43	Superior facial height (n-pr)	87	78	68	68	90	76	99	100	80
14	49	Superior facial breadth (fmt-fmt)	117	97	86	100	117	107	100	108	107
15	50	Bi-orbital breadth (ek-ek)	89	84	78	89	100	99	101	93	82
16	52	Bizygomatic breadth (zy-zy)	157	126	102	117	–	135	153	165	143
17		Zygomatic breadth index (14/16 × 100)	75	74	84	85	–	84	–	65	74
18	53	Bimaxillary breadth (zm-zm)	–	103	84	97	113	105	126	119	106
19	55	Interorbital breadth (mf-mf)	18	19	20	27	24	25	23	24	24
20	56	Orbital breadth (mf-ek)	38	36	31	33	39	39	36	37	33
21	57	Orbital height (perpendicular to 20)	34	32	31	31	33	36	41	33	30
22	71	Nasal bridge length (n-rhi)	–	27	26	18	20	18	35	30	28
23	73	Nasal bridge breadth superior	–	5	8	8	8	13	12	14	11
24		Nasal bridge breadth at anterior lacrimal crests	–	11	5	10	–	24	19	11	–
25	74	Nasal bridge breadth inferior	–	11	13	11	10	18	11	7	8
26		Nasal bridge height (nasion subtense at anterior lacrimal crests)	–	4	9	8	–	9	4	5	–
27	69	Nasal height (n-ns)	58	50	49	45	57	52	72	64	54
28	70	Nasal aperture height (rhi-ns)	29	26	22	28	39	30	38	35	24
29	68	Maximum nasal aperture width	23	23	26	25	27	32	30	31	25
30		Orbitoalveolar height (or-alveolar plane)	55	53	44	47	59	51	53	69	57
31	60	Malar thickness	14	13	13	8	–	12	20	18	18
32		Infraorbital foramen height (to inferior orbital margin)	–	12	15	15	14	16	30	25	26
33		Prosthion to zygomaxillare (pr-zm)	–	67	57	55	69	67	80	82	71
34		Prosthion to zygoorbitale (pr-zyo)	–	60	50	57	75	70	73	81	69
35		Masseter origin height index (33/34 × 100)	–	112	104	96	92	96	110	101	103
36	47	Subnasale to prosthion (horizontal projection)	28	23	13	19	17	16	23	27	26
37	48	Subnasal to prosthion (vertical projection)	15	21	17	18	30	21	12	25	22
38		Subnasale projection index (36/37 × 100)	187	108	76	106	57	79	192	108	122
39	94	Incisor alveolar length	–	13	16	15	14	16	15	15	13
40	96	Premolar alveolar length	–	15	18	16	16	13	21	22	17

continued on next page

Item	Measurement description in (6)	Measurement	*Au. afarensis*	*Au. africanus*	*Au. sediba*	*H. habilis*	*H. rudolfensis*	*H. erectus*	*Au. aethiopicus*	*Au. boisei*	*Au. robustus*
41	98	Intercanine distance	26	30	30	30	33	31	–	29	27
42	88	Palate breadth (ekm-ekm)	68	64	63	70	80	66	83	82	67
43	141	Mandibular symphysis height	39	38	32	27	36	34	–	47	42
44	142	Mandibular symphysis depth	60	20	19	19	24	19	–	28	25
45	147	Mandibular corpus height at P_4	34	33	28	30	38	30	–	42	38
46	148	Mandibular corpus depth at P_4	19	21	18	20	22	19	–	28	24
47	149	Cross-sectional area at P_4 (calculated as an ellipse)	511	558	382	427	653	458	–	910	709
48	150	Mandibular corpus height at M_1	33	32	28	29	36	30	35	41	37
49	151	Mandibular corpus depth at M_1	19	21	18	20	23	20	26	28	26
50	152	Cross-sectional area at M_1 (calculated as an ellipse)	488	532	396	421	667	469	715	913	759
51	154	Mandibular corpus height at M_2	31	31	25	31	36	30	–	41	35
52	155	Mandibular corpus depth at M_2	22	25	22	23	26	21	–	31	28
53	156	Cross-sectional area at M_2 (calculated as an ellipse)	536	612	436	537	745	504	–	980	770
54	162	Height of mental foramen relative to alveolar margin	20	19	13	13	17	13	–	20	20
55		Maxillary incisor crown area (I^1+I^2)	143	135	109	132	137	136	–	117	109
56		Maxillary canine crown area	107	104	79	95	118	96	–	76	79
57		Maxillary postcanine crown area	713	868	731	755	829	617	–	1012	941
58		Mandibular canine crown area	87	95	68	83	–	79	–	72	61
59		Mandibular molar crown area	550	651	536	565	668	466	–	781	678
60		Maxillary incisor to postcanine ratio	20.0	15.6	14.9	17.4	16.6	22.1	–	11.5	11.6
61		Maxillary canine to postcanine ratio	15.0	11.9	10.8	12.6	14.2	15.5	–	7.5	8.4
62		Mandibular canine to molar ratio	15.8	14.6	12.7	14.6	–	16.7	–	9.2	9.0

to the facial plane. The face is mesognathic. The palate is consistently deep along its entire extent, with a parabolic dental arcade.

Mandible. Descriptions apply to the more complete juvenile (MH1) mandible unless otherwise stated. The nearly vertical mandibular symphysis presents a weak lateral tubercle, resulting in a slight mental trigone, and a weak mandibular incurvation results in a slight *mentum osseum*. The post-incisive planum is weakly developed and almost vertical. Both mandibular corpora are relatively gracile, with a low height along the alveolar margin. The extramolar sulcus is relatively narrow in both mandibles. In MH1, a moderate lateral prominence displays its greatest protrusion at the mesial extent of M_2, with a marked decrease in robusticity to P_4; in MH2 the moderate lateral prominence shows its greatest protrusion at M_3, with a marked decrease in robusticity to M_2. The alveolar prominence is moderately deep with a notable medial projection posteriorly. The anterior and posterior subalveolar fossae are continuous. The ramus of MH1 is tall and narrow, with nearly parallel, vertically oriented anterior and posterior borders; the ramus of MH2 is relatively broader, with nonparallel anterior and posterior borders (fig. S2). The mandibular notch is relatively deep and narrow in MH1 and more open in MH2. The coronoid extends farther superiorly than the condyle. The condyle is mediolaterally broad and anteroposteriorly narrow. The endocondyloid buttress is absent in MH1, whereas in MH2 a weak endocondyloid buttress approaches the condyle without reaching it.

Dental size and proportions. The dentition of the juvenile (MH1) is relatively small, whereas preserved molars of the adult (MH2) are even smaller (Fig. 3 and fig. S4). For MH1, the maxillary central incisor is distinguishable only from the reduced incisors of *Au. robustus*. The maxillary canine is narrower than all canines of *Au. africanus* except TM 1512, whereas the mandibular canine falls well below the range of *Au. africanus*. Premolars and molars are at the lower end of the *Au. africanus* range and within that of *H. habilis–H. rudolfensis* and *H. erectus*. Molar dimensions of the adult individual (MH2) are smaller than those of *Au. africanus*, are at or below the range of those of *H. habilis–H. rudolfensis*, and are within the range of those of *H. erectus*. *Au. sediba* mirrors the *Au. africanus* pattern of maxillary molars that increase slightly in size posteriorly, though it differs in that the molars tend to be considerably larger in the latter taxon. Conversely, the *Au. sediba* pattern varies slightly from that seen in specimens KNM-ER 1813, OH 13, and OH 65 and *H. erectus*, wherein the molars increase from M^1 to M^2 but then decrease to M^3. In broad terms, the teeth of *Au. sediba* are similar in size to teeth of specimens assigned to *Homo* but share the closely spaced cusp apices seen in *Australopithecus.*

Postcranium. Preserved postcranial remains of *Au. sediba* (table S1) denote small-bodied

hominins that retain an australopith pattern of long upper limbs, a high brachial index, and relatively large upper limb joint surfaces (table S2). In addition to these aspects of limb and joint proportions, numerous other features in the upper limb are shared with sibling species of *Australopithecus* (to the exclusion of later *Homo*), including a scapula with a cranially oriented glenoid fossa and a strongly developed axillary border; a prominent conoid tubercle on the clavicle, with a pronounced angular margin; low proximal-to-distal humeral articular proportions; a distal humerus with a marked crest for the brachioradialis muscle, a large and deep olecranon fossa with a septal aperture, and a marked trochlear/capitular keel (*19*); an ulna with a pronounced flexor carpi ulnaris tubercle; and long, robust, and curved manual phalanges that preserve strong attachment sites for the flexor digitorum superficialis muscle.

Numerous features of the hip, knee, and ankle indicate that *Au. sediba* was a habitual biped. In terms of size and morphology, the proximal and distal articular ends of the femur and tibia fall within the range of variation of specimens attributed to *Au. africanus.* However, several derived features in the pelvis link the Malapa specimens with later *Homo.* In the os coxa (Fig. 4), *Au. sediba* shares with *Homo* a pronounced acetabulocristal buttress; a more posterior position of the cristal tubercle; a superoinferiorly extended posterior iliac blade, with an expanded retroauricular area; a sigmoid-shaped anterior inferior iliac spine; a reduced lever arm for weight transfer between the auricular surface and the acetabulum; an enlarged and rugose iliofemoral ligament attachment area; a tall and thin pubic symphyseal face; and a relatively short ischium with a deep and narrow tuberoacetabular sulcus. These features are present in taxonomically unassigned postcranial remains from Koobi Fora (KNM-ER 3228) and Olduvai Gorge (OH 28), which have been argued to represent early *Homo* (*20*), as well as in early *Homo erectus* (*21*). An os coxa from Swartkrans (SK 3155) has been considered by some to also represent early *Homo* (*22*) but can be seen to possess the australopith pattern in most of these features. In addition, *Au. sediba* shares with later *Homo* the human-like pattern of low humeral-to-femoral diaphyseal strength ratios, in contrast to the ape-like pattern seen in the *H. habilis* specimen OH 62 (table S2).

Although aspects of the pelvis are derived, the foot skeleton is more primitive overall, sharing with other australopiths a flat talar trochlea articular surface with medial and lateral margins with equal radii of curvature, and a short, stout, and medially twisted talar neck with a high horizontal angle and a low neck torsion angle

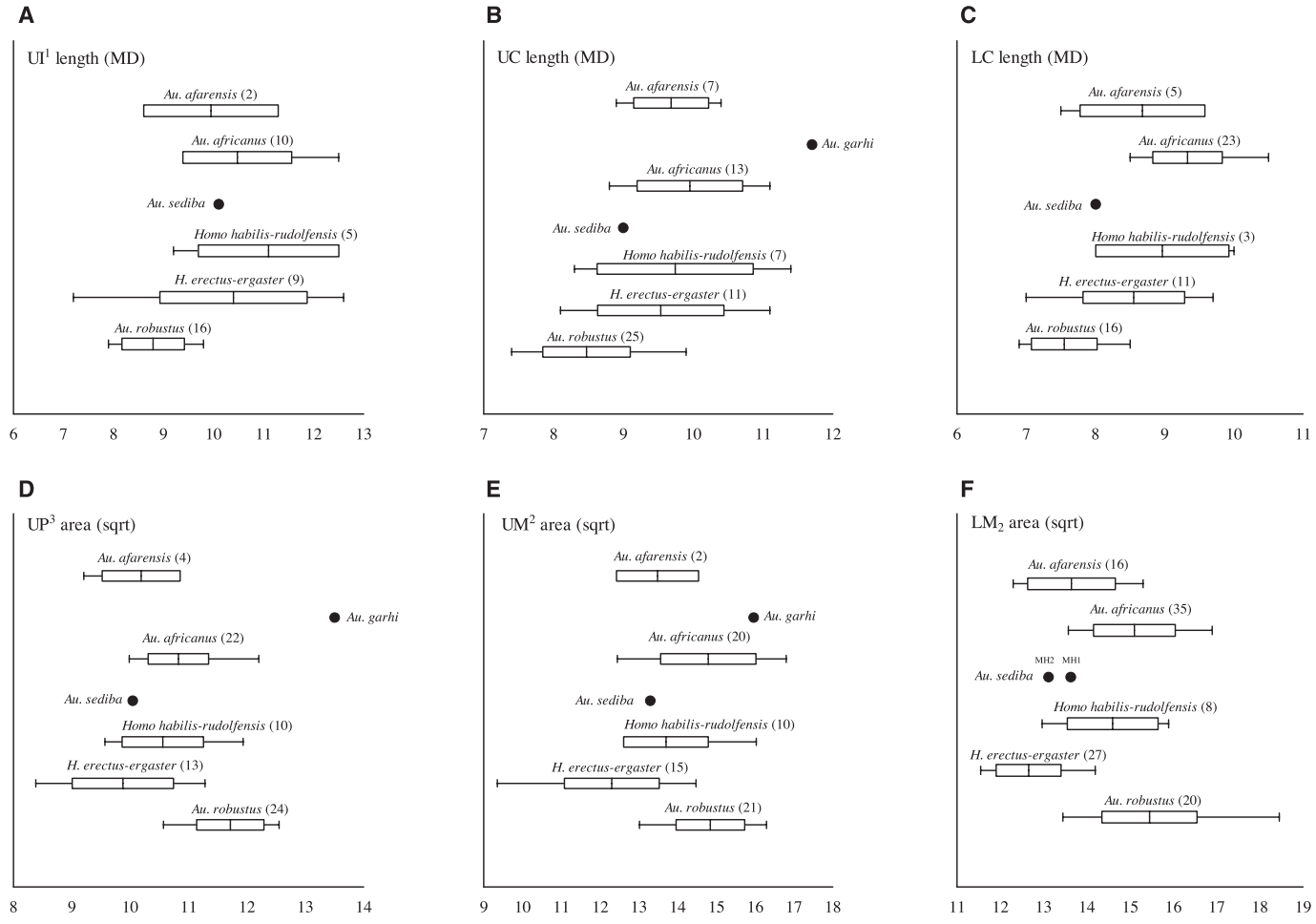

Fig. 3. Dental size of a selection of *Au. sediba* teeth compared to other early hominin taxa; see fig. S4 for additional teeth. Dental measurements were taken as described by Wood (*6*). Owing to small sample sizes, *H. habilis* and *H. rudolfensis* were combined. (**A**) Upper central incisor mesiodistal (MD) length. (**B**) Upper canine MD length. (**C**) Lower canine MD length. (**D**) Square root of calculated [MD × BL (BL, buccolingual)] upper third premolar area. (**E**) Square root of calculated (MD × BL) upper second molar area. (**F**) Square root of calculated (MD × BL) lower second molar area. Measures were taken on original specimens by D.J.D. for *Au. africanus*, *Au. robustus*, and *Au. sediba*. Measurements for *Au. afarensis*, *H. habilis*, *H. rudolfensis*, and *H. erectus* are from (*6*). P^4 is not fully erupted on the right side of MH1, therefore measures of the maxillary postcanine dentition are presented for the left side only. Dental metrics for *Au. sediba* are as follows (MD, BL, in millimeters): Maxillary: MH1: RI1 10.1, 6.9; LI2 7.7 (damaged), 5.1; RC 9.0, 8.8; LP3 9.0, 11.2; LP4 9.2, 12.1; LM1 12.9, 12.0; LM2 12.9, 13.7; LM3 13.3, 14.1; MH2: RM3 11.3, 12.9. Mandibular: MH1: LC 8.0, 8.5; RM1 12.5, 11.6; RM2 14.4, 12.9; RM3 14.9, 13.8; MH2: RM1 11.8, 11.1; RM2 14.1, 12.2; RM3 14.2, 12.7; LM3 14.1, 12.5.

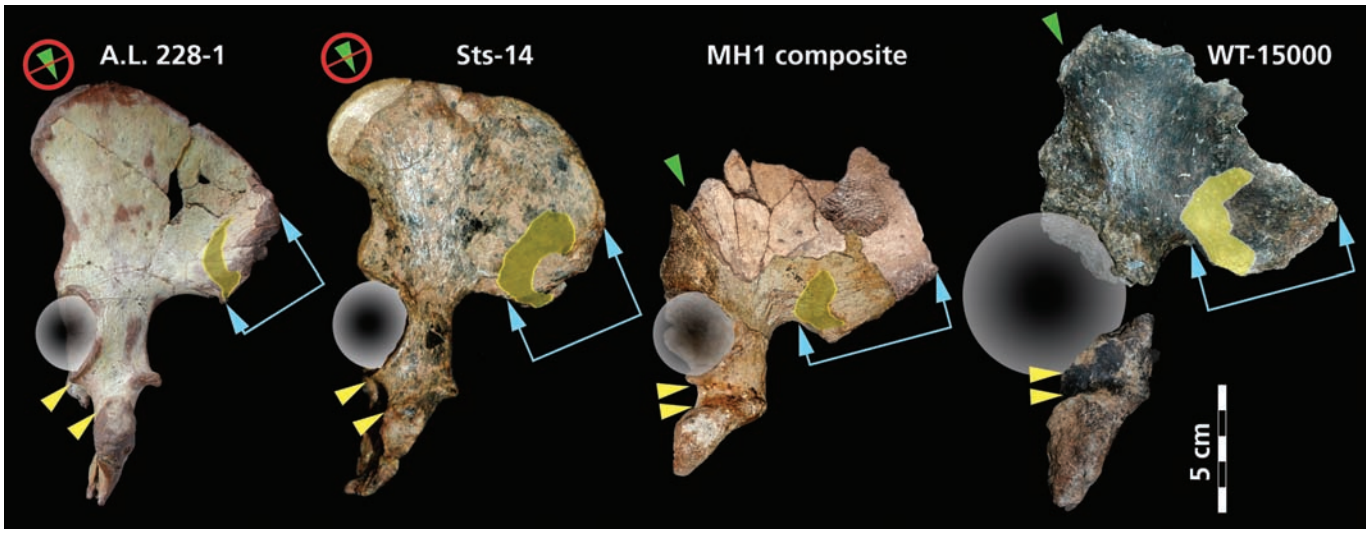

Fig. 4. Representative ossa coxae, in lateral view, from left to right, of *Au. afarensis* (AL 288-1), *Au. africanus* (Sts 14), *Au. sediba* (MH1), and *H. erectus* (KNM-WT 15000). The specimens are oriented so that the iliac blades all lie in the plane of the photograph (which thus leads to differences between specimens in the orientation of the acetabula and ischial tuberosities). MH1 possesses derived, *Homo*-like morphology compared to other australopithecines, including a relative reduction in the weight transfer distance from the sacroiliac (yellow) to hip (circle) joints; expansion of the retroauricular surface of the ilium (blue arrows) (determined by striking a line from the center of the sphere representing the femoral head to the most distant point on the posterior ilium; the superior arrow marks the terminus of this line, and the inferior arrow marks the intersection of this line with the most anterior point on the auricular face); narrowing of the tuberoacetabular sulcus (delimited by yellow arrows); and pronouncement of the acetabulocristal (green arrows) and acetabulosacral buttresses.

(table S2 and fig. S5). The calcaneus is markedly primitive in its overall morphology: the bone is strongly angled along the proximodistal axis, with the point of maximum inflexion occurring at an enlarged peroneal trochlea; the lateral plantar tubercle is lacking; the calcaneal axis is set about 45° to the transverse plane; and the calcaneocuboid facet is vertically set and lacks an expanded posterior projection for the beak of the cuboid (*23*).

Discussion. The age and overall morphology of *Au. sediba* imply that it is most likely descended from *Au. africanus*, and appears more derived toward *Homo* than do *Au. afarensis*, *Au. garhi*, and *Au. africanus*. Elsewhere in South Africa, the Sterkfontein cranium Stw 53, dated to 2.0 to 1.5 Ma, is generally considered to represent either *H. habilis* (*10*, *24*, *25*) or perhaps an undiagnosed form of early *Homo* (*26*). It played an important role in the assignment of OH 62 to *H. habilis* (*27*). However, the derived craniodental morphology of *Au. sediba* casts doubt on the attribution of Stw 53 to early *Homo* [see also (*28*)]: Stw 53 appears to be more primitive than MH1 in retaining closely spaced temporal lines; marked postorbital constriction; a weakly developed supraorbital torus; narrow, nonprojecting nasal bones; anterior pillars; marked nasoalveolar prognathism; medial and lateral expansion of the frontal process of the zygomatic bone; and laterally flared zygomatics. If Stw 53 instead represents *Au. africanus*, the assignment of OH 62 to *H. habilis* becomes tenuous. Attribution of the partial skeleton KNM-ER 3735 to *H. habilis* was tentatively based, in part, on a favorable comparison with OH 62 and on the hypothesis that there were no other contemporaneous non-robust australopith species to which it could be assigned in East Africa (*29*). As a result, the interpretation of KNM-ER 3735 as *H. habilis* also becomes uncertain.

The phylogenetic significance of the co-occurrence of derived postcranial features in *Au. sediba*, *H. erectus*, and a sample of isolated fossils generally referred to *Homo* sp. indet. (table S2) is not clear: The latter might represent early *H. erectus*, it might sample the postcranium of *H. rudolfensis* (which would then imply an evolutionary pathway from *Au. sediba* to *H. rudolfensis* to *H. erectus*), or it might represent the postcranium of *H. habilis* [which would suggest that OH 62 and KNM-ER 3735 (two specimens with ostensibly more primitive postcranial skeletons) do not belong in this taxon]. If the latter possibility holds, it could suggest a phylogenetic sequence from *Au. sediba* to *H. habilis* to *H. erectus*. Conversely, although the overall postcranial morphology of *Au. sediba* is similar to that of other australopiths, a number of derived features of the os coxa align the Malapa hominins with later *Homo* (*H. erectus*) to the exclusion of other australopiths. Additionally, *Au. sediba* shares a small number of cranial traits with *H. erectus* that are not exhibited in the *H. habilis–H. rudolfensis* hypodigm, including slight postorbital constriction and convexity of the infraorbital region (*18*). Following on this, MH1 compares favorably with SK 847 (*H. erectus*) in the development of the supraorbital torus, nasal bones, infraorbital region, frontal process of the zygomatic, and subnasal projection. However, MH1 differs from SK 847 in its relatively smaller size, the robust glabelar region, the weakly developed supratoral sulcus, the steeply inclined zygomaticoalveolar crests with a high masseter origin, and the moderate canine juga, all features aligning MH1 with *Australopithecus*. It is thus not possible to establish the precise phylogenetic position of *Au. sediba* in relation to the various species assigned to early *Homo*. We can conclude that combined craniodental and postcranial evidence demonstrates that this new species shares more derived features with early *Homo* than does any other known australopith species (Table 1 and table S2) and thus represents a candidate ancestor for the genus, or a sister group to a close ancestor that persisted for some time after the first appearance of *Homo*.

The discovery of a <1.95-million-year-old (*16*) australopith that is potentially ancestral to *Homo* is seemingly at odds with the recovery of older fossils attributed to the latter genus (*5*) or of approximately contemporaneous fossils attributable to *H. erectus* (*6*, *30*). However, it is unlikely that Malapa represents either the earliest or the latest temporal appearance of *Au. sediba*, nor does it encompass the geographical expanse that the species once occupied. We hypothesize that *Au. sediba* was derived via cladogenesis from *Au. africanus* (≈3.0 to 2.4 Ma), a taxon whose first and last appearance dates are also uncertain (*31*). The possibility that *Au. sediba* split from *Au. africanus* before the earliest appearance of *Homo* cannot be discounted.

Although the skull and skeleton of *Au. sediba* do evince derived features shared with early *Homo*, the overall body plan is that of a hominin at an australopith adaptive grade. This supports the argument, based on endocranial volume and craniodental morphology, that this species is most parsimoniously attributed to the genus *Australopithecus*. The Malapa specimens dem-

onstrate that the evolutionary transition from a small-bodied and perhaps more arboreal-adapted hominin (such as *Au. africanus*) to a larger-bodied, possibly full-striding terrestrial biped (such as *H. erectus*) occurred in a mosaic fashion. Changes in functionally important aspects of pelvic morphology, including a reduction of the sacroacetabular weight-bearing load arm and enhanced acetabulosacral buttressing (reflecting enhancement of the hip extensor mechanism), enlargement of the iliofemoral ligament attachment (reflecting a shift in position of the line of transfer of weight to behind the center of rotation of the hip joint), enlargement of the acetabulocristal buttress (denoting enhancement of an alternating pelvic tilt mechanism), and reduction of the distance from the acetabulum to the ischial tuberosity (reflecting a reduction in the moment arm of the hamstring muscles) (*20*, *32*) occurred within the context of an otherwise australopith body plan, and seemingly before an increase in hominin encephalization [in contrast to the argument in (*33*)]. Relative humeral and femoral diaphyseal strength measures (table S2) also suggest that habitual locomotor patterns in *Au. sediba* involved a more modern human-like mechanical load-sharing than that seen in the *H. habilis* specimen OH 62 (*34*, *35*). Mosaic evolutionary changes are mirrored in craniodental morphology, because the increasingly wide spacing of the temporal lines and reduction in postorbital constriction that characterize *Homo* first appeared in an australopith and before significant cranial expansion. Moreover, dental reduction, particularly in the postcanine dentition, preceded the cuspal rearrangement (wide spacing of postcanine tooth cusps) that marks early *Homo*.

The pattern of dental eruption and epiphyseal fusion exhibited by MH1 indicates that its age at death was 12 to 13 years by human standards, whereas in MH2 the advanced degree of occlusal attrition and epiphyseal closure indicates that it had reached full adulthood (SOM text S1). Although juvenile, MH1 exhibits pronounced development of the supraorbital region and canine juga, eversion of the gonial angle of the mandible, and large rugose muscle scars in the skeleton, all indicating that this was a male individual. And, although fully adult, the mandible and skeleton of MH2 are smaller than in MH1, which, combined with the less rugose muscle scars and the shape of the pubic body of the os coxa, suggests that MH2 was a female. In terms of dental dimensions, MH1 has mandibular molar occlusal surface areas that are 10.7% (M_1) and 8.1% (M_2) larger than those of MH2. Dimorphism in the postcranial skeleton likewise is not great, though the juvenile status of MH1 tends to confound efforts to assess adult body size. The diameter of the proximal epiphysis for the femoral head of MH1 (29.8 mm) is approximately 9.1% smaller than the superoinferior diameter of MH2's femoral head (32.7 mm). It is likely that MH1 would have experienced some appositional increase in joint size before maturity, thus this disparity would probably have decreased somewhat. The distal humeral epiphysis of MH1 is fully fused and its articular breadth (35.3 mm) is only marginally larger than that of MH2 (35.2 mm). Thus, although the dentition and postcranial skeleton are at odds in the degree of apparent size differences, the overall level of dimorphism, if these sex attributions are correct, appears slight in the Malapa hominins and was probably similar to that evinced by modern humans.

References and Notes

1. R. A. Dart, *Nature* **115**, 195 (1925).
2. D. C. Johanson, T. D. White, *Science* **203**, 321 (1979).
3. B. Asfaw *et al*., *Science* **284**, 629 (1999).
4. M. G. Leakey *et al*., *Nature* **410**, 433 (2001).
5. W. H. Kimbel, D. C. Johanson, Y. Rak, *Am. J. Phys. Anthropol.* **103**, 235 (1997).
6. B. Wood, *Koobi Fora Research Project, Volume 4: Hominid Cranial Remains* (Clarendon Press, Oxford, 1991).
7. G. P. Rightmire, *Am. J. Phys. Anthropol.* **90**, 1 (1993).
8. R. J. Blumenschine *et al*., *Science* **299**, 1217 (2003).
9. B. Wood, M. Collard, *Science* **284**, 65 (1999).
10. P. V. Tobias, *Olduvai Gorge Volume 4: The Skulls, Endocasts and Teeth of* Homo habilis (Cambridge Univ. Press, Cambridge, 1991).
11. D. S. Strait, F. E. Grine, *J. Hum. Evol.* **47**, 399 (2004).
12. D. E. Lieberman, *Nature* **410**, 419 (2001).
13. The *H. erectus* hypodigm includes African specimens that are referred to the taxon *H. ergaster* by some. Unless otherwise stated, we collectively refer to *H. habilis, H. rudolfensis, H. erectus*, and *H. ergaster* materials as "early *Homo*."
14. F. Spoor *et al*., *Nature* **448**, 688 (2007).
15. P. V. Tobias, *The Brain in Hominid Evolution* (Columbia Univ. Press, New York, 1971).
16. P. H. G. M. Dirks *et al*., *Science* **328**, 205 (2010).
17. D. M. Bramble, D. E. Lieberman, *Nature* **432**, 345 (2004).
18. Rak (*36*) describes a feature in the infraorbital region of *Au. boisei* that he refers to as a nasomaxillary basin: a concave depression that is surrounded by a more elevated topography. We see a similar concavity in the infraorbital region of specimens of *H. habilis–H. rudolfensis* (KNM-ER 1470, KNM-ER 1805, KNM-ER 1813, and OH 24), although it is not clear whether they represent homologous structures. In specimens of *Au. africanus, Au. sediba*, and *H. erectus*, we recognize a slight convexity in this area.
19. Some humeri that are probably best attributed to *Australopithecus* lack marked development of the trochlear/capitular keel [or "lateral crest": see (*37*)], and thus the absence of a marked crest does not reliably differentiate *Australopithecus* from *Homo*. However, although some specimens of early *Homo* (such as KNM-WT 15000) have crests that are more strongly developed than those of modern humans, none exhibit the marked crests of the australopiths. Thus, the marked crest seen in the Malapa humeri can be seen to be shared with *Australopithecus* rather than *Homo*.
20. M. D. Rose, *Am. J. Phys. Anthropol.* **63**, 371 (1984).
21. A. Walker, C. B. Ruff, in *The Nariokotome* Homo erectus *Skeleton*, A. Walker, R. E. F. Leakey, Eds. (Harvard Univ. Press, Cambridge, MA, 1993), pp. 221–233.
22. C. K. Brain, E. S. Vrba, J. T. Robinson, *Ann. Transv. Mus.* **29**, 55 (1974).
23. L. C. Aiello, C. Dean, *An Introduction to Human Evolutionary Anatomy* (Academic Press, London, 1990).
24. A. R. Hughes, P. V. Tobias, *Nature* **265**, 310 (1977).
25. D. Curnoe, P. V. Tobias, *J. Hum. Evol.* **50**, 36 (2006).
26. F. E. Grine, W. L. Jungers, J. Schultz, *J. Hum. Evol.* **30**, 189 (1996).
27. D. C. Johanson *et al*., *Nature* **327**, 205 (1987).
28. R. J. Clarke, *S. Afr. J. Sci.* **104**, 443 (2008).
29. R. E. F. Leakey, A. Walker, C. V. Ward, H. M. Grausz, in *Hominidae*, G. Giacobini, Ed. (Jaca Books, Milano, Italy, 1989), pp. 167–173.
30. L. Gabunia, A. Vekua, *Nature* **373**, 509 (1995).
31. T. D. White, in *Paleoclimate and Evolution with Emphasis on Human Origins*, E. S. Vrba, G. H. Denton, T. C. Partridge, L. H. Burckle, Eds. (Yale Univ. Press, New Haven, CT, 1995), pp. 369–384.
32. J. T. Stern Jr., R. L. Susman, *Am. J. Phys. Anthropol.* **60**, 279 (1983).
33. C. O. Lovejoy, *Gait Posture* **21**, 113 (2005).
34. C. Ruff, *Am. J. Phys. Anthropol.* **138**, 90 (2009).
35. It is possible that the more *Homo*-like humeral-to-femoral diaphyseal strength ratios in *Au. sediba* reflect a relative reinforcement of the femoral diaphysis in the context of femoral elongation (resulting in longer bending-moment arms) without a change in locomotor behavior. At present, we are unable to directly assess the absolute and relative length of the femur in *Au. sediba*.
36. Y. Rak, *The Australopithecine Face* (Academic Press, New York, 1983).
37. M. R. Lague, W. L. Jungers, *Am. J. Phys. Anthropol.* **101**, 401 (1996).
38. R. R. Skelton, H. M. McHenry, *J. Hum. Evol.* **23**, 309 (1992).
39. M. Collard, B. Wood, *Proc. Natl. Acad. Sci. U.S.A.* **97**, 5003 (2000).
40. H. F. Smith, F. E. Grine, *J. Hum. Evol.* **54**, 684 (2008).

41. We thank the South African Heritage Resources Agency for the permits to work at the Malapa site; the Nash family for granting access to the Malapa site and continued support of research on their reserve; the South African Department of Science and Technology, the South African National Research Foundation, the Institute for Human Evolution, the Palaeontological Scientific Trust, the Andrew W. Mellon Foundation, the AfricaArray Program, the U.S. Diplomatic Mission to South Africa, and Sir Richard Branson for funding; the University of the Witwatersrand's Schools of Geosciences and Anatomical Sciences and the Bernard Price Institute for Palaeontology for support and facilities; the Gauteng Government, Gauteng Department of Agriculture, Conservation and Environment and the Cradle of Humankind Management Authority; E. Mbua, P. Kiura, V. Iminjili, and the National Museums of Kenya for access to comparative specimens; Optech and Optron; Duke University; the Ray A. Rothrock Fellowship of Texas A&M University; and the University of Zurich 2009 Field School. Numerous individuals have been involved in the ongoing preparation and excavation of these fossils, including C. Dube, B. Eloff, C. Kemp, M. Kgasi, M. Languza, J. Malaza, G. Mokoma, P. Mukanela, T. Nemvhundi, M. Ngcamphalala, S. Jirah, S. Tshabalala, and C. Yates. Other individuals who have given significant support to this project include B. de Klerk, C. Steininger, B. Kuhn, L. Pollarolo, B. Zipfel, J. Kretzen, D. Conforti, J. McCaffery, C. Dlamini, H. Visser, R. McCrae-Samuel, B. Nkosi, B. Louw, L. Backwell, F. Thackeray, and M. Peltier. T. Stidham helped construct the cladogram in fig. S3. J. Smilg facilitated computed tomography scanning of the specimens. R. Clarke and F. Kirera provided valuable discussions on these and other hominin fossils in Africa.

Supporting Online Material

www.sciencemag.org/cgi/content/full/328/5975/195/DC1
SOM Text 1 to 4
Figs. S1 to S5
Tables S1 and S2
References

19 November 2009; accepted 26 February 2010
10.1126/science.1184944